

See discussions, stats, and author profiles for this publication at: <https://www.researchgate.net/publication/24417997>

Hybridization of Genomic DNA Adsorbed Electrostatically onto Cationic Surfaces

ARTICLE in THE JOURNAL OF PHYSICAL CHEMISTRY B · JUNE 2009

Impact Factor: 3.3 · DOI: 10.1021/jp9010636 · Source: PubMed

CITATIONS

9

READS

32

8 AUTHORS, INCLUDING:



A. Nabok

Sheffield Hallam University

112 PUBLICATIONS 1,224 CITATIONS

SEE PROFILE



Anna Tsargorodskaya

The University of Sheffield

25 PUBLICATIONS 364 CITATIONS

SEE PROFILE



Tatiana Berzina

Università degli studi di Parma

89 PUBLICATIONS 1,131 CITATIONS

SEE PROFILE



Luigi Cristofolini

Università degli studi di Parma

95 PUBLICATIONS 790 CITATIONS

SEE PROFILE

Hybridization of Genomic DNA Adsorbed Electrostatically onto Cationic Surfaces

Alexei Nabok,^{*,†} Anna Tsargorodskaya,[†] Damien Gauthier,[†] Frank Davis,[‡]
Seamus P. J. Higson,[‡] Tatiana Berzina,[§] Luigi Cristofolini,[§] and Marco P. Fontana[§]

Materials and Engineering Research Institute, City Campus, Sheffield Hallam University, Howard Street, Sheffield, S1 1WB, U.K., Cranfield Health, Cranfield University, MK43 0AL, U.K., Laboratorio Nanotecnologie Molecolari, Department of Physics, University of Parma, INFN-CNR, CRS-SOFT, 43100 Parma, Italy

Received: February 5, 2009; Revised Manuscript Received: March 26, 2009

Our previous study revealed an intriguing phenomenon of partial hybridization of two single strands of genomic DNA, with one of them being electrostatically adsorbed on a solid surface. Although the effect was confirmed with different methods and even recommended for a crude DNA analysis, the exact mechanism of hybridization was not clear. This work presents the results of more detailed study of adsorption and hybridization of two genomic DNA, of salmon and herring, using the experimental techniques of total internal reflection ellipsometry (TIRE), ATR FTIR spectroscopy, and AFM. The in situ TIRE study of the hybridization kinetics allowed the evaluation of the association constant. It appeared to be in the range of $10^5 \text{ mol}^{-1} \text{ L}$ for binding complementary ss-DNA in comparison to $10^4 \text{ mol}^{-1} \text{ L}$ for binding of noncomplementary ss-DNA. FTIR study directly confirmed the effect of partial binding of complementary ss-DNA by monitoring the 1650 and 1690 cm^{-1} spectral bands. AFM showed the transformation from clearly resolved images of separate chains of ss-DNA molecules adsorbed on the surface of mica to an inhomogeneous layer of tangled and overlapping DNA molecules following binding of another complementary ss-DNA.

Introduction

DNA analysis, one of the greatest achievements of 20th century, has become a routine procedure in many areas of human activity. DNA analysis is defined as an identification of the individual species by detection of a unique sequence of nucleotides (i.e. the genetic code) within the DNA double helix structure. Several experimental techniques are currently available for such analyses, mostly based on the use of optical luminescent markers and special enzymes that can cleave the DNA chain. These technologies are generally expensive because of the requirements for consumables, sophisticated equipment and highly qualified personnel, thus making DNA analysis available only in specialized laboratories. Because of shipment of samples and waiting times for many of these techniques, the analysis procedure becomes time-consuming.

However, industries require relatively fast (albeit crude) methods of DNA analysis; for example, for control of food products, textiles, and other natural raw materials. Development of faster and cheaper methods of DNA analysis is currently the subject of intense research. Recent proposals to achieve this are based on the idea of decomposition of DNA into single strands followed by their reconstruction either in solution or in an adsorbed state.^{1–5} In an ideal scenario, two cDNA single strands (ss) are more likely to form a double helix structure than noncomplementary ss-DNA, which provides a possibility of selective identification of DNA molecules.

This idea was confirmed experimentally in our early works^{4,6} utilizing genomic DNA of two species of fish, herring and salmon, in which ss-DNA was adsorbed electrostatically on a solid surface and then exposed again to a solution of ss-DNA.

Qualitative proof was obtained first by electrochemical impedance and conventional spectroscopic ellipsometry measurements.⁴ More detailed study using a novel technique of total internal reflection ellipsometry (TIRE)^{7,8} revealed a substantial increase in the adsorbed layer thickness (of about 20 nm) when complementary ss-DNA was adsorbed (herring-on-herring or salmon-on-salmon), whereas much smaller effects (in the range of 2–4 nm) were observed in the case of adsorption of noncomplementary ss-DNA (herring-on-salmon or salmon-on-herring).⁶

Such a unique observation was quite difficult to grasp because an ideal hybridization of two long ss-DNA strands, one of them adsorbed on the surface, represents a very unlikely process. Whereas genomic DNA denatures to form single-stranded DNA by heating, hybridization back to the double-stranded form is a complex process, since genomic DNA contains a wide variety of individual chains with different lengths and sequences. Even when DNA from a single species is allowed to reassociate, measurements have shown that the nucleotide pairing is imprecise.⁹ The extent of reassociation between DNA of different species has been shown to be a measure of the phylogenealogy between the species.¹⁰ In the adsorbed state, most likely a partial hybridization occurs, meaning that DNA first adsorbs as a random coil which is accompanied by tangling and overlapping of DNA molecules on the surface to form a multilayer film.⁸ There is also the possibility of some of the hybridization occurring in solution before adsorption, and it is possible that such behavior is a contributing factor to the adsorption observed. However, double-stranded DNA formed in solution would be less likely to adsorb, since it could not undergo hybridization reactions with the initially adsorbed layer of ss-DNA. This is borne out by the fact that when non-cDNA stands are utilized as a control experiment, levels of adsorption are much lower.

* To whom correspondence should be addressed. Phone: +44 114 2256905. Fax: +44 114 2253433. E-mail: a.nabok@shu.ac.uk.

[†] Sheffield Hallam University.

[‡] Cranfield University.

[§] University of Parma.

Other workers have reported that deposition of single-stranded DNA onto amino-silanized glass gave surfaces capable of selective hybridization of cDNA, although whether actual formation of a DNA double helix occurs is still in doubt, and it is possible that a nonhelical duplex may be the preferred structure.³ Our earlier observed increases in the layer thickness of 20 nm are far larger than the diameter of DNA double strand (ds) of about 2.5 nm; this is a clear indication of the formation of a multilayer of DNA chains. Other workers have also demonstrated formation of multilayers of single-stranded genomic calf thymus DNA using quartz crystal microbalance studies.¹¹ It appears that this partial hybridization is less likely in the case of adsorption of noncomplementary ss-DNA, resulting in a smaller increase in the layer thickness. Although the obtained results were quite convincing, further investigation is required to prove the mechanism of partial hybridization of ss-DNA on the surface utilizing complementary experimental techniques. The evaluation of the kinetics of DNA hybridization will also help in this investigation.

In this work, we present the results of further study of DNA hybridization using spectroscopic ellipsometry in TIRE configuration for adsorption kinetics tests with subsequent evaluation of the association constant. FTIR spectroscopy was also utilized to distinguish between two forms of DNA (ss and ds) in an adsorbed state. Finally, AFM provided the means for direct observation of ss-DNA on the surface and the subsequent transformations caused by hybridization.

Experimental Details

Sample Preparation. Two types of genomic DNA of herring and salmon (from Sigma Aldrich, Catalogue nos. D6898 and D1626, respectively) were selected for this work. The salmon DNA contains mainly molecules of 2000 bp, whereas the herring DNA molecular contents varied from 300 to 1000 bp. Phosphate buffer (pH 7) was made by dissolving $\text{NaH}_2\text{PO}_4 \cdot \text{H}_2\text{O}$ (0.55 g), $\text{Na}_2\text{HPO}_4 \cdot 12\text{H}_2\text{O}$ (2.11 g), and NaCl (7.73 g) in water and diluting to 1 L. Decomposition of DNA into single strands was carried out by heating the solution of 0.2 mg mL^{-1} DNA in phosphate buffer up to 95°C . Then the sample was sharply cooled in ice-cold water. Samples were then placed into the solution or it was injected and then allowed during the course of adsorption to warm up to room temperature. The solutions were then used for deposition immediately, since the hybridization process and subsequent formation of DNA double strands (ds) begins after cooling, and previous studies show this process to be almost complete after 2 hours. Polyethylenimine (PEI), molecular weight 50 000 and other chemicals were supplied by Sigma (Poole, U.K.).

Three types of solid substrates were used in this work: (i) Cr/Au-coated glass slides for TIRE measurements were prepared by consecutive (without breaking the vacuum) thermal evaporation of layers of Cr (3–4 nm) and Au (20–30 nm) onto clean microscopic glass slides in a vacuum of about 10^{-6} Torr using an Edwards A360 evaporation system. The presence of the Cr underlayer improves the adhesion of the gold to the glass. (ii) ZnSe prisms for ATR-FTIR measurements. (iii) Freshly cleaved mica for the AFM studies.

To give the surface of gold and ZnSe a positive surface charge, these were modified with a layer of polyethylenimine by dipping the samples into a 2 mg mL^{-1} solution of PEI for 15 min, followed by rinsing thoroughly with deionized water (Millipore; Bellerica, MA) to remove loosely bound polycations. The surface of freshly cleaved mica was used as it is, since other workers have reported that networks of calf thymus DNA

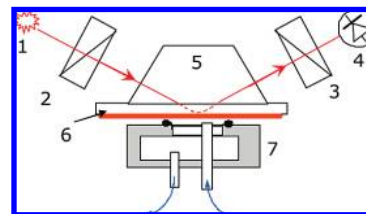


Figure 1. The scheme of TIRE measurements: light source (1), polarizers (2, 3), photodetector (4), 68° prism (5), Cr/Au-coated glass slide (6), and cell (7).

can spontaneously assemble on mica.¹² To deposit the first layer of ss-DNA onto gold or ZnSe, substrates were placed into 0.2 mg mL^{-1} DNA solutions for 15 min. The ss-DNA monolayer is immobilized by electrostatic interaction between the anionic phosphate groups and the cationic PEI, as is found to occur for a wide range of oppositely charged polyelectrolytes. This process of polyelectrolyte self-assembly has been extensively reviewed.^{13,14} Further deposition of a second layer on ZnSe crystals was performed by placing the prism into a 0.2 mg mL^{-1} ss-DNA solution for 2 h.

To observe individual DNA molecules, they were deposited in the surface of mica from diluted ($0.2 \mu\text{g mL}^{-1}$) solutions of either ds- or ss-DNA as before and rinsed.

Experimental Methods. The kinetics of adsorption and hybridization of DNA were studied using spectroscopic ellipsometry. A M2000 V (J. A. Woollam; Lincoln, NE) spectroscopic instrument was employed for this purpose. The modification of the experimental setup described in detail previously^{6,8} allows these measurements in the regime of total internal reflection with the benefits of an enhanced sensitivity and experimental conveniences of Kretschmann SPR (surface plasmon resonance) configuration.¹⁵ As shown schematically in Figure 1a, the light enters the sample (gold-coated glass slide with the DNA layers adsorbed on top of the gold) through the prism; the cell attached underneath allows for the measurements in different media (including liquids).

Biochemical reactions on the surface of gold, including the adsorption and hybridization of DNA (in our case), can be monitored *in situ* by injecting the required solutions into the cell and subsequently recording a number of spectra of two ellipsometric parameters of Ψ and Δ after a certain time interval. Ψ and Δ represent, respectively, the ratio of amplitudes of p- and s-components of polarized light ($\tan \Psi = A_p/A_s$) and the phase shift between them ($\Delta = \varphi_p - \varphi_s$). The data can then be presented as time dependencies of values of Ψ or Δ at selected wavelengths. Such measurements were performed by injecting the solutions of ss-DNA of different concentrations: 0.2, 0.1, 0.05, and 0.02 mg mL^{-1} . Evaluation of the association constant for DNA hybridization $K_A = r_a/r_d$, defined as a ratio of rates of adsorption (r_a) and desorption (r_d), can be performed by fitting the TIRE kinetics data to an integral absorption equation following the procedure described in details in refs 16 and 17.

The IR spectra of DNA layers deposited onto a PEI-modified ZnSe prism were recorded using a Jasco model 420 FTIR spectrometer (JASCO Europe; Capri, Italy) in attenuated total reflection (ATR) mode. The dimensions of the ZnSe 45° trapezoidal prism were $80 \times 10 \times 4 \text{ mm}$. The ATR-FTIR measurements were carried out in a wavenumber range of $4000\text{--}600 \text{ cm}^{-1}$ with 4 cm^{-1} resolution; the spectra were averaged over 128 scans. To eliminate the spectral contribution of water vapors, the sample compartment was purged with a constant flow of dry nitrogen gas. A spectrum from the blank ZnSe prism recorded under identical conditions was subtracted.

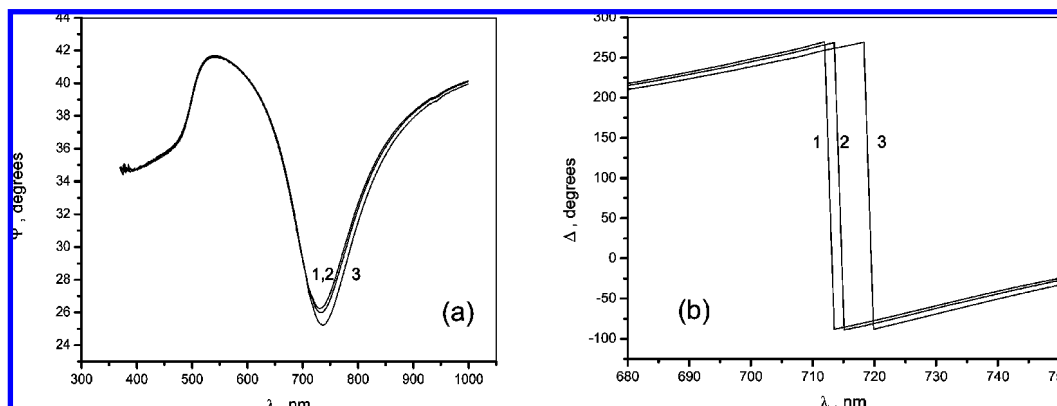


Figure 2. Typical series of $\Psi(\lambda)$ (a) and $\Delta(\lambda)$ (b) spectra illustrating the adsorption of ds-DNA: initial bare gold surface (1), after adsorption of PEI (2), and after adsorption of herring ds-DNA (3).

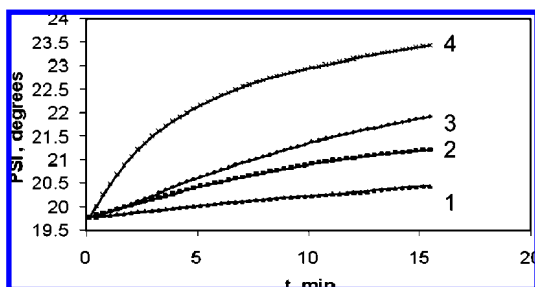


Figure 3. Typical TIRE kinetics for adsorption of complementary (salmon-on-salmon) ss-DNA of different concentrations: 0.01 (1), 0.05 (2), 0.1 (3), and 0.2 mg mL⁻¹ (4).

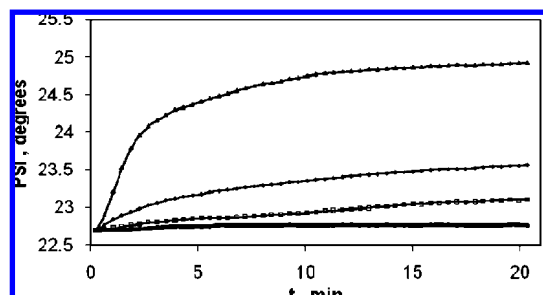


Figure 4. Typical TIRE kinetics for adsorption of noncomplementary (herring-on-salmon) ss-DNA of different concentrations: 0.01 (1), 0.05 (2), 0.1 (3), and 0.2 mg mL⁻¹ (4).

AFM morphology studies of DNA layers deposited on mica were carried out using a Nanoscope IIIa (Digital Instruments) apparatus. Tapping-mode AFM images were recorded with a typical scan rate of 1 Hz. Veeco tapping mode cantilevers with typical oscillation frequency of around 300 kHz and tip radius of about 10 nm were used.

Experimental Results and Discussion

TIRE study. Typical $\Psi(\lambda)$ and $\Delta(\lambda)$ experimental spectra corresponding to consecutive adsorption steps of PEI and ds-DNA are shown in Figure 2

$\Psi(\lambda)$ spectra display distinctive features similar to SPR curves with the maximum and minimum corresponding, respectively, to the critical point of total internal reflection and SPR. The shift of $\Psi(\lambda)$ spectra to larger wavelengths is caused by adsorption of layers of PEI and ds-DNA. In contrast, the $\Delta(\lambda)$ spectra show characteristic sharp drops in phase from 270° to -90° near plasmon resonance. The values of spectral shift are much larger than those for $\Psi(\lambda)$ spectra, which leads to higher sensitivity of the parameter Δ (as compared to Ψ) to molecular adsorption.¹⁸

Since the spectral changes in the film thickness due to the adsorption of the second layer of ss-DNA were studied previously,⁶ the main focus of this work is on kinetics, with TIRE measurements being performed at different concentrations of ss-DNA. The kinetics study of ss-DNA adsorption was carried out, and typical results are presented in Figures 3 and 4 as time dependences of Ψ at a fixed wavelength near the plasmon resonance.

The concentration of ss-DNA in the second adsorption stage was the parameter in this study. Parameters of k_a and k_d can be obtained from the time dependences of Ψ changes ($\Psi\delta$) in

TABLE 1: Parameters for ss-DNA adsorption kinetics

adsorption sequence of ss-DNA	adsorption kinetics parameters		
	adsorption rate, k_a (mol ⁻¹ L s ⁻¹)	desorption rate, k_d (s ⁻¹)	association constant, K_A (mol ⁻¹ L)
salmon-salmon	1.1×10^4	3.3×10^{-2}	3.5×10^5
salmon-herring	5.2×10^2	1.5×10^{-2}	3.5×10^4
herring-herring	1.4×10^4	2.2×10^{-2}	6.0×10^5
herring-salmon	2.3×10^3	4.9×10^{-2}	4.7×10^4

Figure 3 applying the integral adsorption equation as described in refs 8, 16, and 17.

$$\delta\Psi = \frac{k_a C \Psi\delta_{\max}}{k_a C + k_d} \{1 - \exp[-(k_a C + k_d)t]\} \quad (1)$$

where $\Psi\delta_{\max}$ is the maximal value of $\Psi\delta$ (at saturation) and C is the concentration of ss-DNA in solution. These dependencies plotted in semilogarithmic coordinates $\ln \Psi\delta$ vs t appear to be linear with the gradient of $S = k_a C + k_d$. Finally, a linear plot of S vs C yields the values of adsorption and desorption rates k_a and k_d as linear coefficient and intercept, respectively; then the association constant is calculated as their ratio: $K_A = k_a/k_d$. The obtained values of k_a , k_d , and K_A are summarized in Table 1.

As demonstrated, there is an order of magnitude difference between the K_A values for adsorption of complementary ss-DNA and noncomplementary ss-DNA. Such a difference is substantial but not dramatic, and it implies that adsorption of DNA is occurring in both cases, though more pronounced in the case of complementary ss-DNA molecules. The control experiments utilizing non-cDNA display some adsorption of DNA that can be due to a variety of effects, including the partial

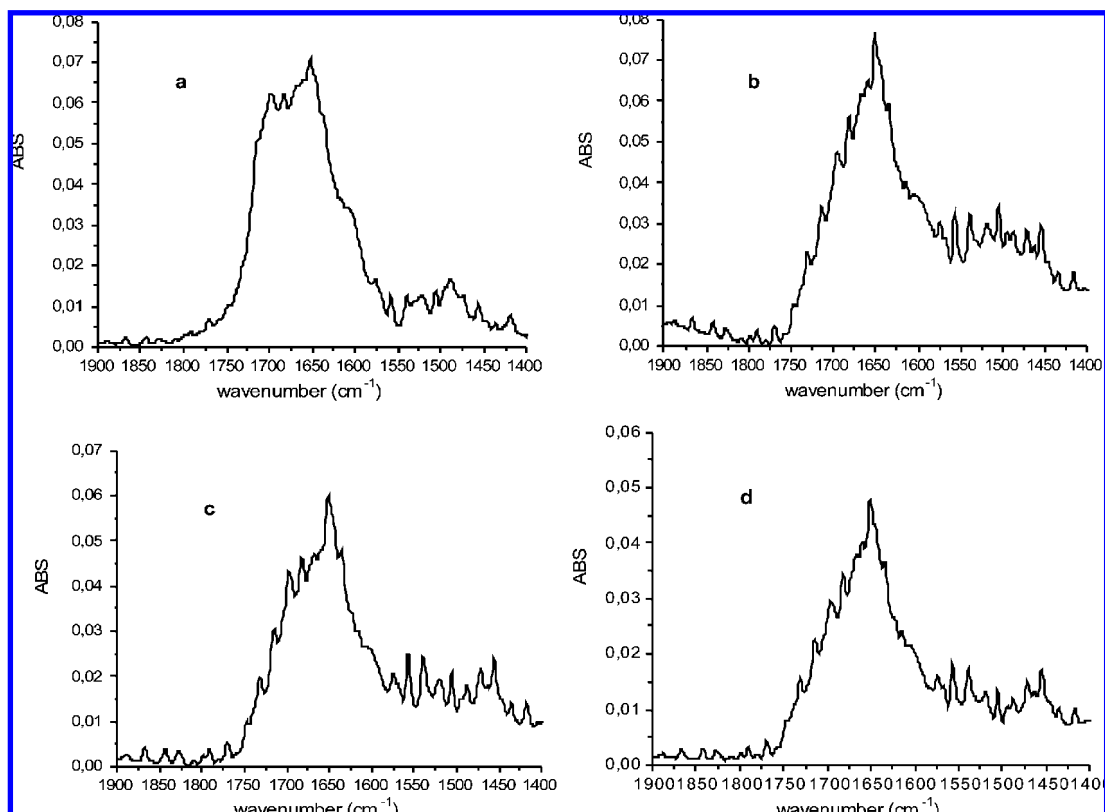


Figure 5. ATR-FTIR spectra of adsorbed DNA layers: salmon ds-DNA (a), salmon ss-DNA (b), salmon ss-DNA on salmon ss-DNA (c), herring ss-DNA on salmon ss-DNA (d).

hybridization of matching portions of the DNA strands or other factors, such as simple physisorption. However, the increased rates and thicker films formed by adsorption of complementary ss-DNA show that even for genomic DNA, hybridization of complementary strands is the major driving force for adsorption. In addition, the obtained values of K_A in the range of 10^4 – 10^5 mol⁻¹ L clearly show that the binding of the second ss-DNA is quite specific but not as high as in the case of immune reactions,⁸ typically having a K_A in the range of 10^7 mol⁻¹ L.

FTIR Measurements. The results of the ATR-FTIR study are shown in Figure 5. We have focused on the bands in the 1650–1690 cm⁻¹ range, corresponding to carbonyl stretches originating in the DNA bases.¹⁶ Another possibly interesting spectral range (about 1450 cm⁻¹) was not analyzed due to the very poor signal-to-noise ratio. In an extensive review¹⁹ of DNA IR spectra, previous authors report that the change between single- and double-stranded DNA structures is most easily visualized by monitoring the C=O stretch vibrations of the guanine and thymine bases, since these appear to be the most affected by base pairing interactions. In the spectrum of ds-DNA adsorbed on the surface (see Figure 6a), both guanine- and thymine-related bands are present. The peak at 1690 cm⁻¹ is indicative of the presence of guanine and thymine bases paired with their respective counterparts²⁰ and, therefore, of a double-helix DNA structure. However in the spectrum of an ss-DNA layer adsorbed on the surface (Figure 5b), the spectral line at 1650 cm⁻¹ dominates, since the effect of base pairing is minimal, and only peaks due to free bases are detected.¹⁹

As one can see from Figure 5c, adsorption of a second layer of complementary ss-DNA (salmon-on-salmon or herring-on-herring) has resulted in a slight increase in the intensity of the 1650 cm⁻¹ line due to adsorption of ss-DNA molecules. The line at 1690 cm⁻¹ has also appeared as a definite shoulder, indicating partial formation of a double strand. In the case of

adsorption of noncomplementary ss-DNA (herring-on-salmon or salmon-on-herring, see Figure 6d), the line at 1690 cm⁻¹ is less pronounced, indicating a low probability of the formation of a double strand. The above results confirm the idea of partial hybridization of two complementary single strands of DNA. It has to be noted, however, that experimental IR spectra exhibit a quite poor signal-to-noise ratio due to a very small actual absorption signal. This makes the data analysis critically dependent on methodological choices. Therefore, the spectra we presented have been corrected only for the blank substrate background; the subtraction of the PEI layer contribution resulted in unacceptable fluctuations. The raw spectrum of the PEI layer is given in the Supporting Information. This problem requires further investigation with higher-quality IR spectra; however, we feel that for the purpose of this paper, the results of Figure 5 provide qualitative support to the partial hybridization idea.

AFM Study. Tapping mode AFM images in Figure 6 clearly show bundles of ds-DNA as well as separate strands of ss-DNA molecules adsorbed on the surface of mica from their respective 0.2 μg mL⁻¹ solutions. These results are similar to those reported earlier,^{12,20} although observed on much longer strands of genomic DNA adsorbed on freshly cleaved and not a chemically modified surface of mica. The observation of molecules of ss-DNA is particularly striking, considering the small dimensions (cross section) of a single oligonucleotide chain. The observed width of the ss-DNA chain of about 20 nm is obviously enlarged because of the finite radius of the tip (see the scheme in Figure 6d). The sharpness of images in Figure 6a, b also indicate that both ds- and ss-DNA are firmly adsorbed to the mica surface.

The adsorption of another layer of ss-DNA on top results in distorted, blurred images, such as shown in Figure 6c, most likely due to the tangling and overlapping of DNA strands on the surface and the formation of a loosely bound 3D DNA

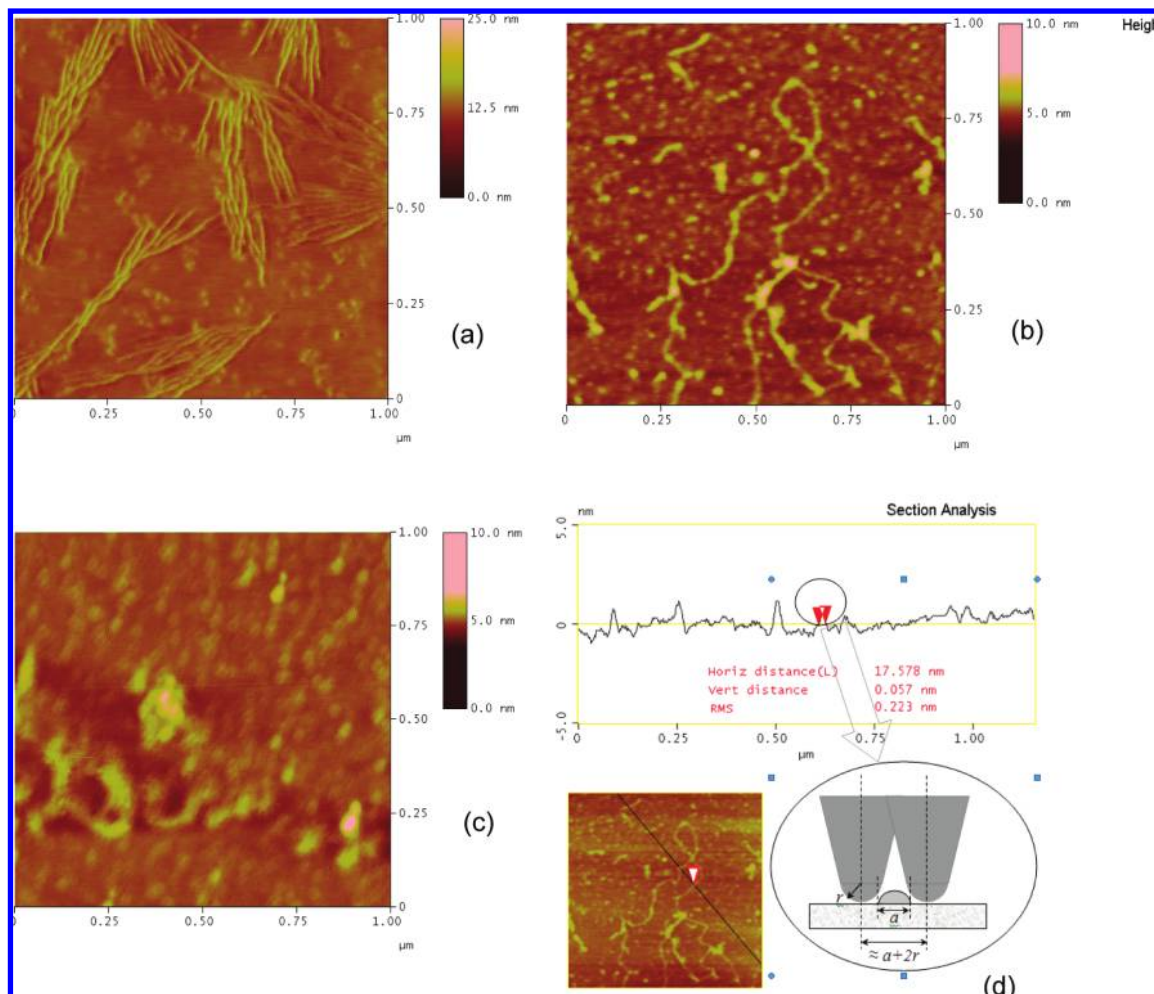


Figure 6. Typical AFM tapping mode images of DNA layers adsorbed on mica: herring ds-DNA (a), herring ss-DNA (b), second adsorption of herring ss-DNA (c), line scan across ss-DNA molecule, results of section analysis and the scheme of features' lateral size enlargement due to a finite tip radius (d).

structure. There is little difference between AFM images taken after adsorption of complementary or noncomplementary ss-DNA. Similar experiments¹² by other workers have shown that calf thymus ds-DNA will assemble to form networks on mica surfaces, and they report heights greater than expected for simple adsorbed monolayers, which they also attribute to overlap and tangling of the polymer chains.

Conclusions

The recent TIRE study confirmed once again the high sensitivity of TIRE measurements, particularly $\Delta(\lambda)$ spectra, to small changes in optical density of adsorbed layers. The use of TIRE in an adsorption kinetics study allowed further progress in understanding of the DNA hybridization mechanism. The evaluation of the association constant showed that binding of complementary ss-DNA chains is about an order of magnitude more specific than for noncomplementary ones. Such a noticeable but not dramatic difference is another indication that the hybridization of DNA is partial in both cases. FTIR measurements confirmed independently that partial binding of ss-DNA is taking place on the surface; it is slightly more pronounced in the case of binding of complementary ss-DNA strands than that for the noncomplementary ones. Direct observation of DNA molecules adsorbed on the surface of mica using tapping mode AFM showed dramatic distortion of initially clear images of ss-DNA chains after a second adsorption of either complemen-

tary or noncomplementary ss-DNA. It is believed this is due to partial hybridization accompanied by tangling and overlapping of DNA chains.

Acknowledgment. The authors thank the British Council for financial support of collaboration between the Universities of Parma (Italy) and Sheffield Hallam (U.K.) through the British–Italian Partnership Programme 2007–2008.

Supporting Information Available: An FTIR spectrum of the PEI layer deposited onto a ZnSe prism is provided here. This information is available free of charge via the Internet at <http://pubs.acs.org>.

References and Notes

- (1) Nicollini, C.; Erokhin, V.; Facci, P.; Guerzoni, S.; Ross, A.; Pashkevich, P. *Biosens. Bioelectron.* **1997**, *12*, 613–618.
- (2) Mascini, M.; Palchetti, H.; Marazza, G. *J. Anal. Chem.* **2001**, *369*, 15–21.
- (3) Lemesko, S. V.; Powdrill, T.; Belosludsev, Y. Y.; Hogan, M. *Nucleic Acids Res.* **2001**, *29*, 3051–3058.
- (4) Davis, F.; Nabok, A. V.; Higson, S. P. *J. Biosens. Bioelectron.* **2005**, *20*, 1531–1538.
- (5) Cristofolini, L.; Berzina, T.; Erokhin, V.; Tenti, M.; Fontana, M. P.; Erokhina, S.; Kononov, O. *Colloids Surf., A* **2008**, *321*, 158–162.
- (6) Nabok, A. V.; Tsargorodskaya, A.; Davis, F.; Higson, S. P. *J. Biosens. Bioelectron.* **2007**, *23*, 377–383.
- (7) Arvin, H.; Poksinski, M.; Iohansen, K. *Appl. Opt.* **2004**, *43*, 3028–2036.

- (8) Nabok, A. V.; Tsargorodskaya, A.; Hassan, A. K.; Starodub, N. F. *Appl. Surf. Sci.* **2005**, *246*, 381–386.
- (9) Britten, R. E.; Kohne, D. E. *Science* **1968**, *161*, 529–540.
- (10) Martin, M. A.; Hoyer, B. H. *Biochemistry* **1966**, *5*, 2706–2713.
- (11) Rawle, R. J.; Selassie, C. R. D.; Johal, M. S. *Langmuir* **2007**, *23*, 9563–9566.
- (12) Zhao, F.; Xu, J. K.; Liu, S. F. *Thin Solid Films* **2008**, *516*, 7555–7559.
- (13) Decher, G. *Science* **1997**, *277*, 1232–1237.
- (14) Schonhoff, M. *Curr. Opin. Colloid Interface Sci.* **2003**, *8*, 86–95.
- (15) Kretschmann, E. *Z. Phys.* **1971**, *241*, 313–324.
- (16) Karlsson, R.; Michaelsson, A.; Mattsson, L. *J. Immunol. Methods* **1991**, *145*, 229–240.
- (17) Liu, X.; Wei, J.; Song, D.; Zhang, Z.; Zhang, H.; Luo, G. *Anal. Biochem.* **2003**, *314*, 301–309.
- (18) Nabok, A. V.; Tsargorodskaya, A. *Thin Solid Films* **2008**, *516*, 8993–9001.
- (19) Banyay, M.; Sarkar, M.; Graslund, A. *Biophys. Chem.* **2003**, *104*, 477–488.
- (20) Rippe, K.; Mucke, N.; Langowski, J. *Nucleic Acids Res.* **1997**, *25*, 1736–1744.

JP9010636